The Isothermal Section of the Phase Diagram of Mg-Co-Ga Ternary System

Nazar Pavlyuk[1] · Grygoriy Dmytriv[1] · Volodymyr Pavlyuk[1,2] · Sylvio Indris[3] · Helmut Ehrenberg[3]

Abstract The isothermal section of the phase diagram of the Mg-Co-Ga ternary system at 200 °C for the full composition range was built. The formation of five ternary compounds was observed. The crystal structures of all ternary compounds: τ_1—$MgCo_2Ga_5$ (own structure type, *Pnnm* space group), τ_2—$Mg_3Co_2Ga_7$ (*C2/c* space group, own structure type), τ_3—$MgCoGa_2$ (*P*2_1/*n* space group, own structure type), τ_4—$Mg_{1-x}Co_{2-y}Ga_{x+y}$ (x = 0.06, y = 0.64) (*Cmcm* space group, own structure type), τ_5—$Mg_{1-x}Co_{2-y}Ga_{x+y}$ (x = 0.10, y = 0.16) (*R*-3 *m* space group, own structure type) were investigated by means of single crystal diffraction. In addition to ternary compounds, solid solutions based on binary phases are formed in the system. The solid solution $MgCo_{2-x}Ga_x$ (x = 0-1, *P*6_3/*mmc* space group, $MgZn_2$ structure type) represent the largest area of homogeneity. The phase content of alloys was determined by SEM/EDX analysis.

Keywords crystal structure · experimental study · isothermal section · magnesium alloys · phase equilibria

✉ Nazar Pavlyuk
nazar.pavlyuk@gmail.com

[1] Department of Inorganic Chemistry, Ivan Franko National University of Lviv, Lviv, Ukraine

[2] Institute of Chemistry, Jan Długosz University, Częstochowa, Poland

[3] Institute for Applied Materials (IAM), Karlsruhe Institute of Technology (KIT), Eggenstein-Leopoldshafen, Germany

1 Introduction

Recently, interest in magnesium alloys has been growing due to their use in various industries. Among them is the production of light and ultra-light alloys, as well as materials for the accumulation and storage of hydrogen, and electrode materials in ion-magnesium batteries.[1 4]

As it is known, Mg-Co-Ga phase diagram was not described fully earlier, only crystal structure data for five ternary phases partially described earlier by one of the authors.[5 8] The first one is $MgCo_2Ga_5$ phase, which is orthorhombic (*Pnnm* space group, own $MgCo_2Ga_5$-type) with following cell parameters: a = 6.2486, b = 6.6652, c = 6.0523 Å. Detailed information on this phase was published together with that of isostructural $MgNi_2Ga_5$.[5] The second one is monoclinic $Mg_3Co_2Ga_7$ (*C2/c* space group, own $Mg_3Co_2Ga_7$ structure type, a = 9.0873, b = 9.4598, c = 9.4361 Å, β = 93.605(8)°) and crystal structure details was reported in.[6] Crystal structure of the third compound $MgCoGa_2$ was solved and refined in both space groups as *P*2_1/*c* (standard setting) and *P*2_1/*n* (non-standard setting). The refined lattice parameters for standard setting are: a = 5.1505(2) Å, b = 7.2571(2) Å, c = 8.0264(3) Å, β = 125.571(3); for non-standard setting: a = 5.1505 (2) Å, b = 7.2571 (2) Å, c = 6.5464 (2) Å, β = 94.217 (3)°.[7] The crystal structure of new $MgCo_{2-x}Ga_x$ (x = 1.0), $Mg_{1-x}Co_{2-y}Ga_{x+y}$ (x = 0.06, y = 0.64) and $Mg_{1-x}Co_{2-y}Ga_{x+y}$ (x = 0.10, y = 0.16) Laves phases from Mg-Co-Ga system have been recently published.[8]

Given the literature data,[5 8] which indicate the formation of ternary intermetallics in the Mg-Co-Ga system, prompted us to study the system in the full range of compositions. This will make it possible to establish the composition regions of the existence of ternary compounds

and the boundaries of solid solutions based on binary phases.

In this contribution we report experimental results of the investigation of isothermal section of the Mg-Co-Ga ternary system phase diagram at 473 K for the full composition region and crystal structure data for unpublished solid solution phases.

2 Literature Data on Boundary Binary Diagrams

The assessed versions of Mg-Ga, Ga-Co and Mg-Co phase diagrams were described by Massalski[9] (Fig. 1. They are the result of an evaluation of the experimental data from the literature[10 15]). For Mg-Ga system, five binary phases, Mg_2Ga_5, $MgGa_2$, MgGa, Mg_2Ga and Mg_5Ga_2, were reported. In the case of Co-Ga, two binary phases, CoGa and $CoGa_3$, were reported. In Mg-Co only one binary phase, Co_2Mg, was reported. The crystal structure data for the binary Mg-Ga, Ga-Co, Mg-Co systems is given in Table 1.

Thermodynamic assessments were conducted using experimental phase diagram data of the Ga–Co, Mg-Co and Mg-Ga systems by means of CALPHAD (Calculation of Phase Diagrams) approach.[16 18] The calculated results agree well with the experimental data from the literature.

3 Experimental Details

All samples (60 alloys) were synthesized by induction melting in arc-sealed Ta crucibles to prevent any evaporation of constituting compounds with subsequent composition shift. They were afterwards annealed inside quartz ampoules under vacuum at 200 °C for two weeks. Magnesium (chips, 6-35 mesh, 99.98% trace metals basis, Sigma-Aldrich Chemie GmbH), cobalt (powder, < 150 μm, $\geq 99.9\%$ trace metals basis, Sigma-Aldrich Chemie GmbH) and gallium (99.99% trace metals basis, Sigma-Aldrich Chemie GmbH) were used as the starting materials. The annealing temperature was chosen based on the melting temperature of pure components, binary phases, and eutectics. It should be noted that gallium has a very low melting temperature (29.7 °C), and that in the Mg-Ga and Co-Ga binary systems, low-melting eutectics (28-30 °C) exist.[9] At higher annealing temperatures the liquid region would extend in a ternary system. To avoid this, a temperature at which all phases, except the sold Ga phase, exist in a solid state was chosen.

The x-ray powder diffraction (XRPD) of the samples was carried out using STOE STADI P and RIGAKU Mini Flex D-600 powder diffractometers with Mo Kα- and Cu Kα-radiation, respectively. TESCAN Vega3 Scanning Electron Microscopy (SEM) and Energy-Dispersive x-Ray Analysis (EDX, Oxford Instruments energy dispersive x-ray analyzer, Aztec ONE system) were used to determine the number of phases and their qualitative and quantitative chemical compositions.

X-ray single crystal diffraction was used for detailed crystal structure refinement of the solid solutions. A single crystal was first checked by Laue and rotation methods (camera RKV-86, Mo and Cu-radiation) to determine its symmetry and suitability for x-ray intensity data collection. The intensity data were collected by an automatic four-circle Xcalibur Oxford Diffraction diffractometer with CCD detector (graphite monochromatized Mo–Kα radiation). Scans were taken in the ω mode, the analytical absorption corrections were made by CrysalisRed[19] The crystal structure was solved by direct methods and refined using the SHELX-97 program package.[20]

4 Results and Discussion

4.1 Isothermal Section at 200 °C of the Mg-Co-Ga System

According to previous literature data,[5 8] Mg-Co-Ga system was not investigated in the full composition region. In this article we present the isothermal section at 200 °C of the Mg-Co-Ga system studied in the full composition range (Fig. 2). The nominal compositions of the prepared alloys are marked on the isothermal section of phase diagram which is presented in Fig. 2. The results of SEM/EDX and XRPD characterization of selected samples are listed in Table 2. The secondary electron images of some Mg-Co-Ga alloys are presented in Fig. 3 and 4. The results of phase analysis of some x-ray powder patterns are presented in Fig. 5-8.

The Mg-Co-Ga isothermal section at 200 °C is characterized by several ternary phases and various solid solutions based on binary phases of the boundary systems. Generally, some of them have a wide homogeneity region, that give rise to many broad two-phase fields. The

Fig. 1 Phase diagram of Ga-Mg, Co-Ga and Co-Mg binary systems. Redrawn from[9]

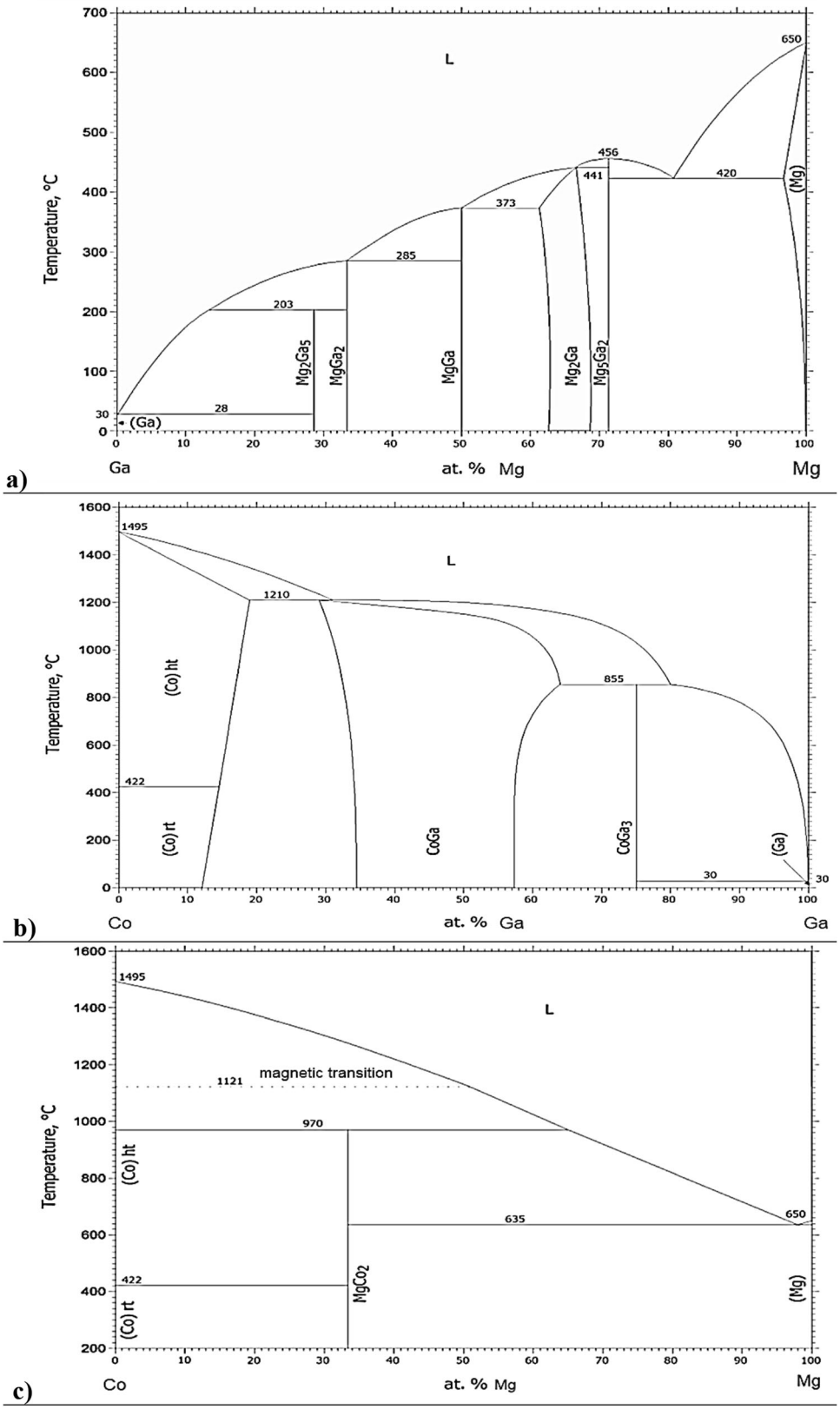

Table 1 Mg-Co-Ga solid phases

Formula	Entry prototype / Pearson symbol	SG symbol	Lattice parameters, Å			References
			a	*b*	*c*	
$MgCo_2$	$MgZn_2$, *hP*12	$P6_3/mmc$	4.859	…	7.954	9, 15
MgCo	GdNi, *cF*96	*Fd*-3 *m*	11.434	…	…	9, 15
Mg_5Ga_2	own, *oI*28	*Ibam*	7.017	13.708	6.020	10, 13
Mg_2Ga	own, *hP*18	*P*-62*c*	7.794	…	6.893	10, 13
MgGa	own, *tI*32	$I4_1/a$	10.530	…	5.530	10, 13
$MgGa_2$	$CaIn_2$, *hP*6	$P6_3/mmc$	4.343	…	6.982	10, 13
Mg_2Ga_5	own, *tI*28	*I*4/*mmm*	8.627	…	7.111	10, 13
CoGa	CsCl, *cP*2	*Pm*-3 *m*	2.875	…	…	9, 14
$CoGa_3$	$IrIn_3$, *tP*16	$P4_2/mnm$	6.2300	…	6.4312	9, 14
S_1—$MgCo_{2\ x}Ga_x$	$MgZn_2$, *hP*12	$P6_3/mmc$	5.0151(5)	…	8.1086(9)	This work
S_2—$MgGa_{1\ x}Co_x$	MgGa, *tI*32	$I4_1/a$	10.5989(9)	…	5.5511(11)	This work
S_3—$MgGa_{2\ x}Co_x$	$CaIn_2$, *hP*6	$P6_3/mmc$	4.337(1)	…	6.980(1)	This work
S_4—$Mg_2Ga_{5\ x}Co_x$	Mg_5Ga_2, *tI*28	*I*4/*mmm*	8.624(1)	…	7.109(1)	This work
S_5—$CoGa_{3\ x}Mg_x$	$IrIn_3$, *tP*16	$P4_2/mnm$	6.2533(10)	…	6.5427(13)	This work
S_6—$CoGa_{1\ x}Mg_x$	CsCl, *cP*2	*Pm*-3 *m*	2.876(3)	…	…	This work
τ_1—$MgCo_2Ga_5$	own, *oP*16	*Pnnm*	6.2486(2)	6.6652(2)	6.0523(2)	This work
τ_2—$Mg_3Co_2Ga_7$	own, *mC*48	*C*2/*c*	9.0873(9)	9.4598(9) β = 93.605(8)°	9.4361(9)	This work
τ_3—$MgCoGa_2$	own, *mP*16	$P2_1/c$	5.1505(2)	7.2571(2) β = 125.571(3)°	8.0264(2)	This work
τ_4—$Mg_{1\ x}Co_{2\ y}Ga_{x+y}$ (x = 0.06, y = 0.64)	own, *oC*72	*Cmcm*	4.9868(9)	25.959(4)	8.0508(11)	This work
τ_5—$Mg_{1\ x}Co_{2\ y}Ga_{x+y}$ (x = 0.10, y = 0.16)	own, *hR*18	*R*-3 *m*	4.9296(2)	…	12.0744(7)	This work

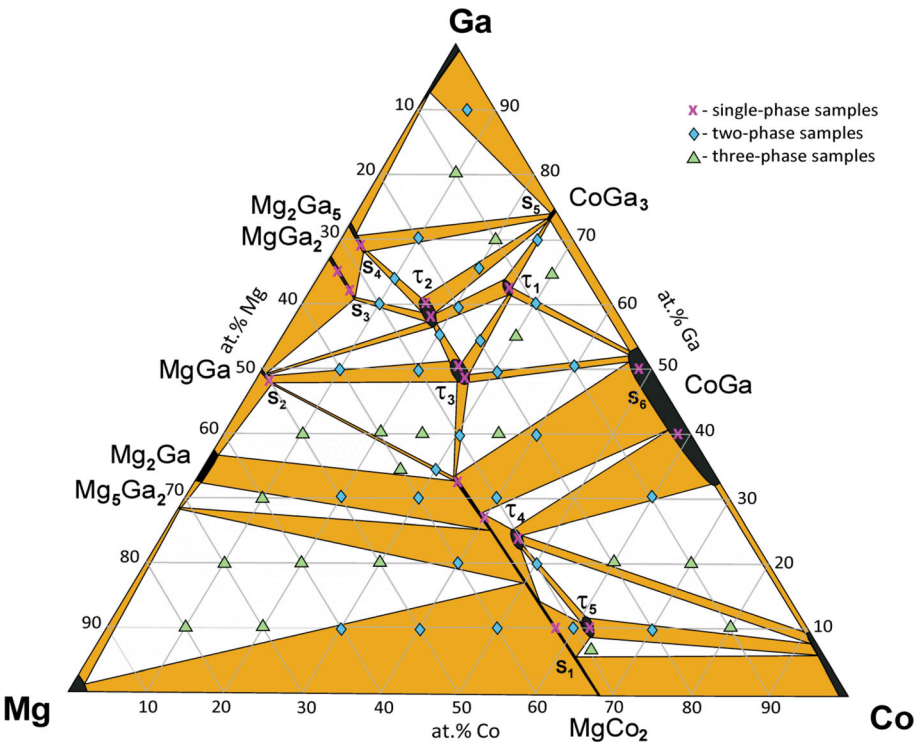

Fig. 2 Isothermal section of the Mg-Co-Ga system at 200 °C and gross compositions of the analyzed alloys

Table 2 Nominal compositions and XRPD data of selected Mg–Co–Ga alloys annealed at 200 °C

Nominal composition	Phases	Compositions by EDXS [at%] Mg; Co; Ga	Entry prototype / Pearson symbol	Lattice parameters, Å		
				a	*b*	*c*
$Mg_{80}Co_{10}Ga_{10}$	Mg	99.5; 0.3; 0.2	Mg, *hP*2	3.2122(1)	…	5.2134(1)
	S_1	33.2; 33.4;33.4	$MgZn_2$, *hP*12	5.078(1)	…	8.194(1)
	Mg_5Ga_2	71.3; 0.2; 28.5	Mg_5Ga_2,oI28	7.018(2)	13.707(6)	6.022(2)
$Mg_{60}Co_{10}Ga_{30}$	S_1	33.2; 33.4;33.4	$MgZn_2$, *hP*12	5.077(1)	…	8.195(2)
	Mg_5Ga_2	71.2; 0.3; 28.5	Mg_2Ga_5, *oI*28	7.017(1)	13.708(2)	6.021(1)
	Mg_2Ga	66.1; 0.7; 33.2	Mg_2Ga, *hP*18	7.851(2)	…	6.942(3)
$Mg_{50}Co_{40}Ga_{10}$	Mg	99.5; 0.3; 0.2	Mg, *hP*2	3.2123(1)	…	5.2134(2)
	S_1	33.2; 33.4;33.4	$MgZn_2$, *hP*12	5.078(1)	…	8.194(1)
$Mg_{50}Co_{30}Ga_{20}$	S_1	33.3; 34.2;32.5	$MgZn_2$, *hP*12 Mg_2	5.0790(2)	…	8.1951(3)
	Mg_5Ga_2	71.4; 0.3; 28.3	Ga_5, *oI*28	7.018(3)	13.707(4)	6.020(2)
	Mg	99.4; 0.3; 0.3	Mg, *hP*2	3.213(1)	…	5.214(1)
$Mg_{40}Co_{10}Ga_{50}$	S_2	50.2; 4.2; 45.6	MgGa, *tI*32	10.530(2)	…	5.526(1)
	τ_3	25.2; 24.9; 49.9	own, *mP*16	5.1505(2)	7.2571(2)	6.5464(2)
					β = 94.217(3)	
$Mg_{35}Co_{30}Ga_{35}$	S_1	33.5; 33.7; 32.8	$MgZn_2$, *hP*12	5.079(1)	…	8.195(2)
	S_2	50.1; 2.2; 47.7	MgGa, *tI*32	10.531(3)	…	5.528(2)
$Mg_{33}Co_{57}Ga_{10}$	S_1	33.5; 56.7; 9.8	$MgZn_2$, *hP*12	4.8902(2)	…	8.0341(3)
$Mg_{33}Co_5Ga_{62}$	S_3	33.5;6.8; 59.7	$CaIn_2$, *hP*6	4.337(1)	…	6.980(1)
$Mg_{30}Co_{30}Ga_{40}$	S_1,	33.6; 33.2;33.2	$MgZn_2$, *hP*12	4.8902(2)	…	8.0341(3)
	τ_3	25.2; 24.9; 49.9	own, *mP*16	5.151(1)	7.257(2)	6.546(1)
					β = 94.22(2)	
$Mg_{30}Co_{45}Ga_{25}$	τ_4	32.4; 44.4;23.2	own, *oC*72	4.9868(9)	25.959(4)	8.051(1)
$Mg_{30}Co_{60}Ga_{10}$	τ_5	30.1; 60.8; 9.1	own, *hR*18	4.9295(4)	…	12.075(1)
	S_1	33.5; 51.3;15.2	$MgZn_2$, hP12	4.997(3)	…	8.097(3)
$Mg_{30}Co_{10}Ga_{60}$	τ_2	25.2; 15.7; 59.1	own, *mC*48	9.0873(9)	9.4598(9)	9.4361(9)
	S_3	33.2; 5.9; 60.9	$CaIn_2$, *hP*6	4.336(1)	*β* = 93.605(8)	6.979(2)
					…	
$Mg_{25}Co_{15}Ga_{60}$	τ_2	25.1; 15.6; 59.3	own, *mC*48	9.0873(9)	9.4598(9)	9.4361(9)
					β = 93.605(8)	
$Mg_{25}Co_{25}Ga_{50}$	τ_3	25.1; 24.8; 50.1	own, *mP*16	5.1505(2)	7.2571(2)	6.5464(2)
					β = 94.227(3)	
$Mg_{20}Co_{25}Ga_{55}$	τ_1	12.4; 25.1; 62.5	own, *oP*16	6.2486(2)	6.6652 (2)	6.0523(2)
	τ_3	25.0; 24.8; 50.2	own, *mP*16	5.151(1)	7.257(2)	6.546(2)
					β = 94.22(3)	
$Mg_{20}Co_{60}Ga_{20}$	τ_4	32.1; 44.6; 23.3	own, *oC*72	4.987(1)	25.959(3)	8.051(2)
	S_6	1.1; 50.2; 48.7	CsCl, *cP*2	2.876(3)	…	…
	Co	0.1; 99.2; 0.7	Mg, *hP*2	2.508(1)	…	4.079(1)
$Mg_{20}Co_{70}Ga_{10}$	τ_5	30.1; 60.8; 9.1	own, *hR*18	4.9295(4)	…	12.075(1)
	Co	0.1; 99.2; 0.7	Mg, *hP*2	2.508(1)	…	4.079(1)
$Mg_{15}Co_{20}Ga_{65}$	τ_2	25.1; 15.6; 59.3	own, *mC*48	9.0873(9)	9.4598(9)	9.4361(9)
	S_5	2.0; 24.8; 73.2	$IrIn_3$, *tP*16	6.232(2)	*β* = 93.605(8)	6.432(2)
					…	
$Mg_{15}Co_{30}Ga_{55}$	τ_1	12.4; 25.1; 62.5	own, *oP*16	6.2486(2)	6.6652 (2)	6.0523(2)
	τ_3	25.2; 24.7; 50.1	own, *mP*16	5.151(1)	7.257(2)	6.546(2)
	S_6	2.1; 45.5; 52.3	CsCl, cP2	2.914(3)	*β* = 94.22(3)	…
					…	

Table 2 continued

Nominal composition	Phases	Compositions by EDXS [at%] Mg; Co; Ga	Entry prototype / Pearson symbol	Lattice parameters, Å		
				a	*b*	*c*
$Mg_{10}Co_{20}Ga_{70}$	τ_2	25.2; 15.5; 59.3	own, *mC*48	9.087(2)	9.459(3)	9.436(2)
	S_5	0.1; 24.8; 75.1	$IrIn_3$, *tP*16	6.232(2)	β = 93.61(3)	6.432(2)
	S_4	28.4; 4.3; 67.3	Mg_2Ga_5, *oI*28	8.624(1)	…	7.109(1)
					…	
$Mg_5Co_{25}Ga_{70}$	τ_1	12.3; 25.2; 62.5	own, *oP*16	6.248(1)	6.665(1)	6.052(1)
	S_5	0.2; 24.7; 75.1	$IrIn_3$, *tP*16	6.233(1)	…	6.432(2)
$Mg_5Co_{30}Ga_{65}$	τ_1	12.3; 25.2; 62.5	own, *oP*16	6.247(1)	6.664(1)	6.053(1)
	S_5	0.2; 24.7; 75.1	$IrIn_3$, *tP*16	6.233(1)	…	6.432(2)
	S_6	0.1; 50.2; 49.7	CsCl, *cP*2	2.875(2)	…	…

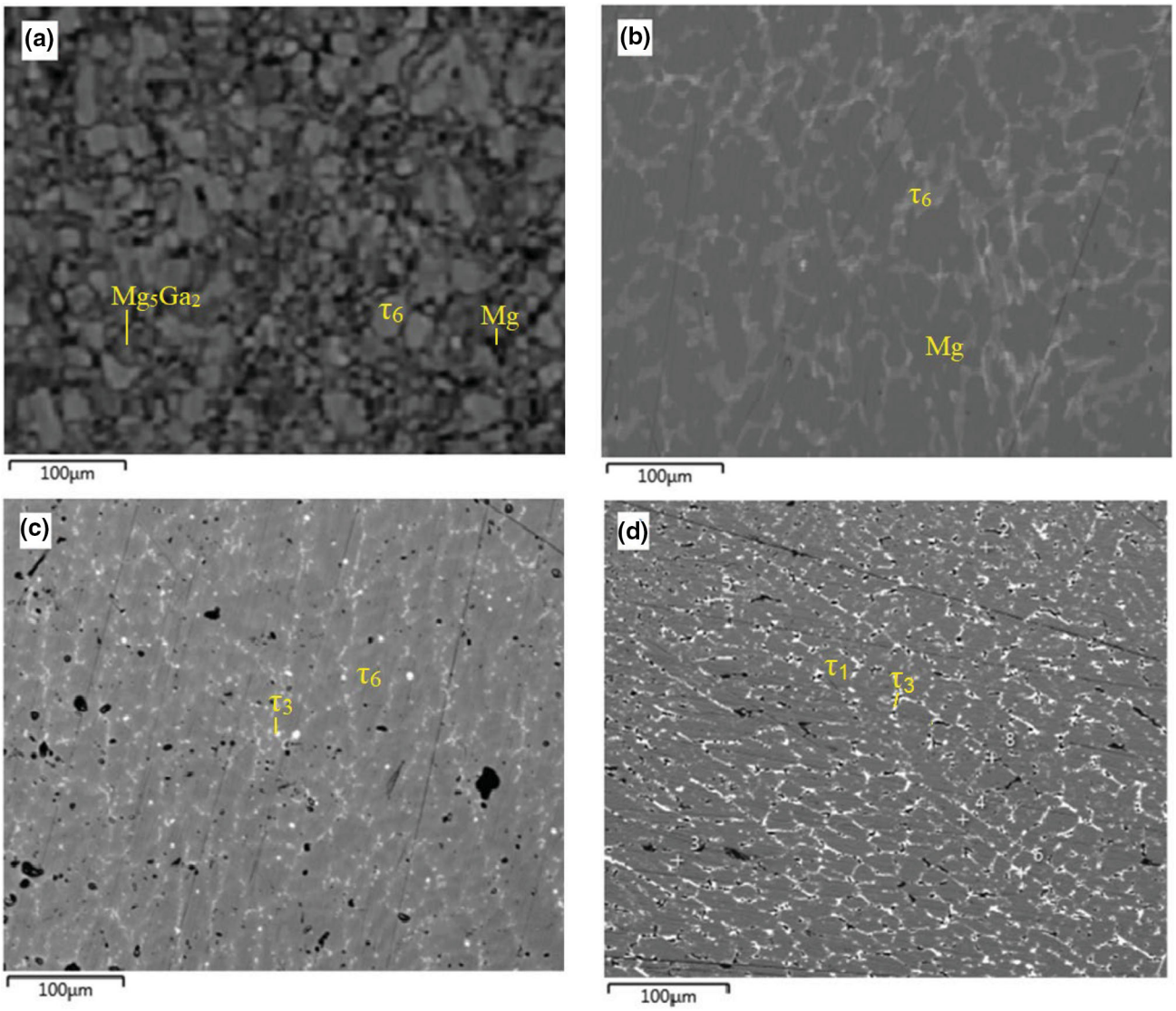

Fig. 3 Micrographs of selected Mg–Co–Ga samples: (a) $Mg_{80}Co_{10}Ga_{10}$ (dark—Mg, grey—τ_6, dark grey—Mg_5Ga_2); (b) $Mg_{50}Co_{40}Ga_{10}$ (dark grey—Mg, grey—τ_6); (c) $Mg_{30}Co_{30}Ga_{40}$ (grey—τ_6, light grey—τ_3); (d) $Mg_{20}Co_{25}Ga_{55}$ (grey—τ_1, light—τ_3)

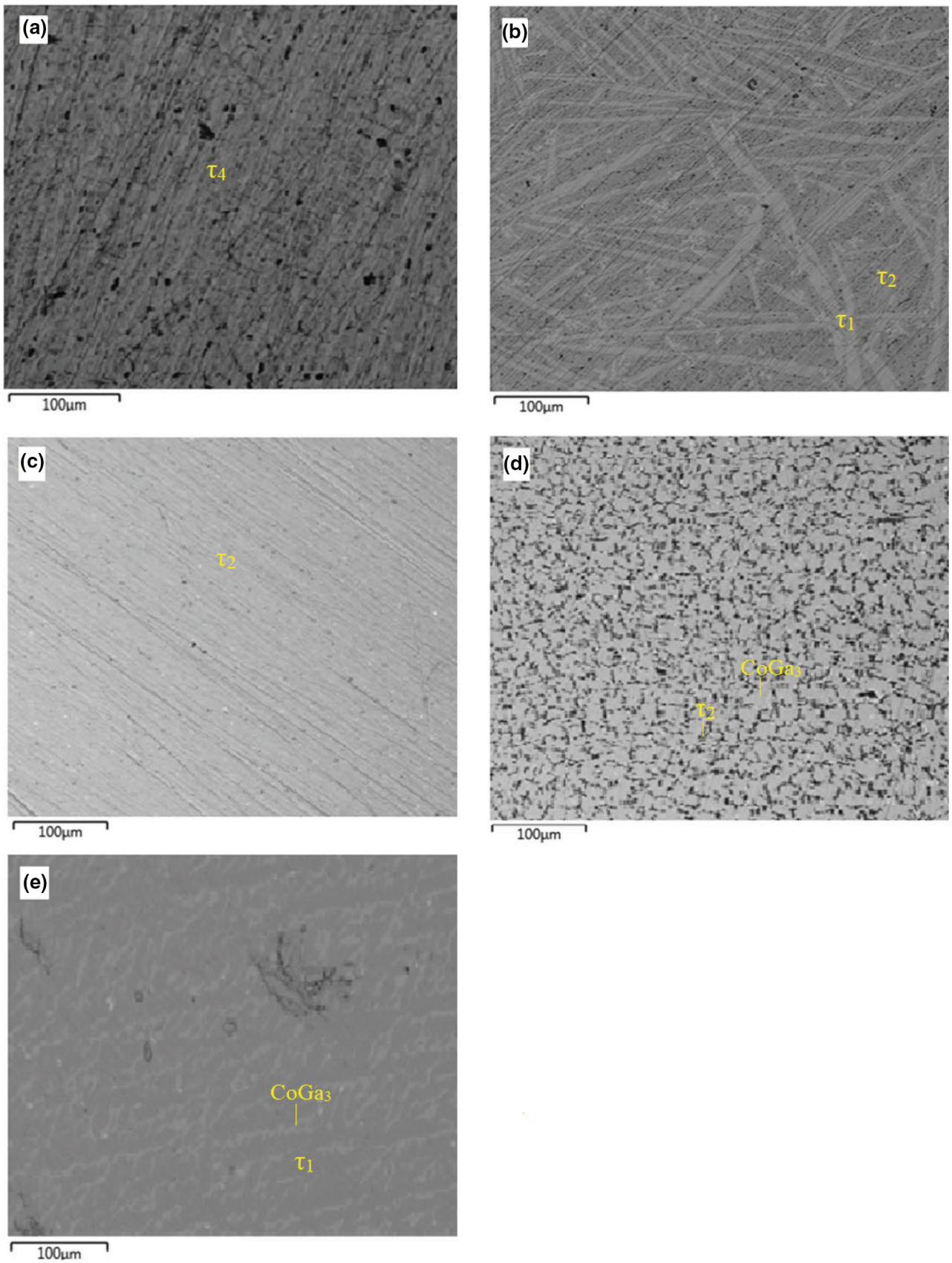

Fig. 4 Micrographs of selected Mg–Co–Ga samples: (a) $Mg_{30}Co_{45}Ga_{25}$ (grey—τ_4); (b) $Mg_{20}Co_{20}Ga_{60}$ (grey—τ_2, light grey—τ_1); (c) $Mg_{25}Co_{15}Ga_{60}$ (light—τ_2); (d) $Mg_{15}Co_{20}Ga_{65}$ (light—$CoGa_3$, grey—τ_2); (e) $Mg_5Co_{25}Ga_{70}$ (light—$CoGa_3$, grey—τ_1)

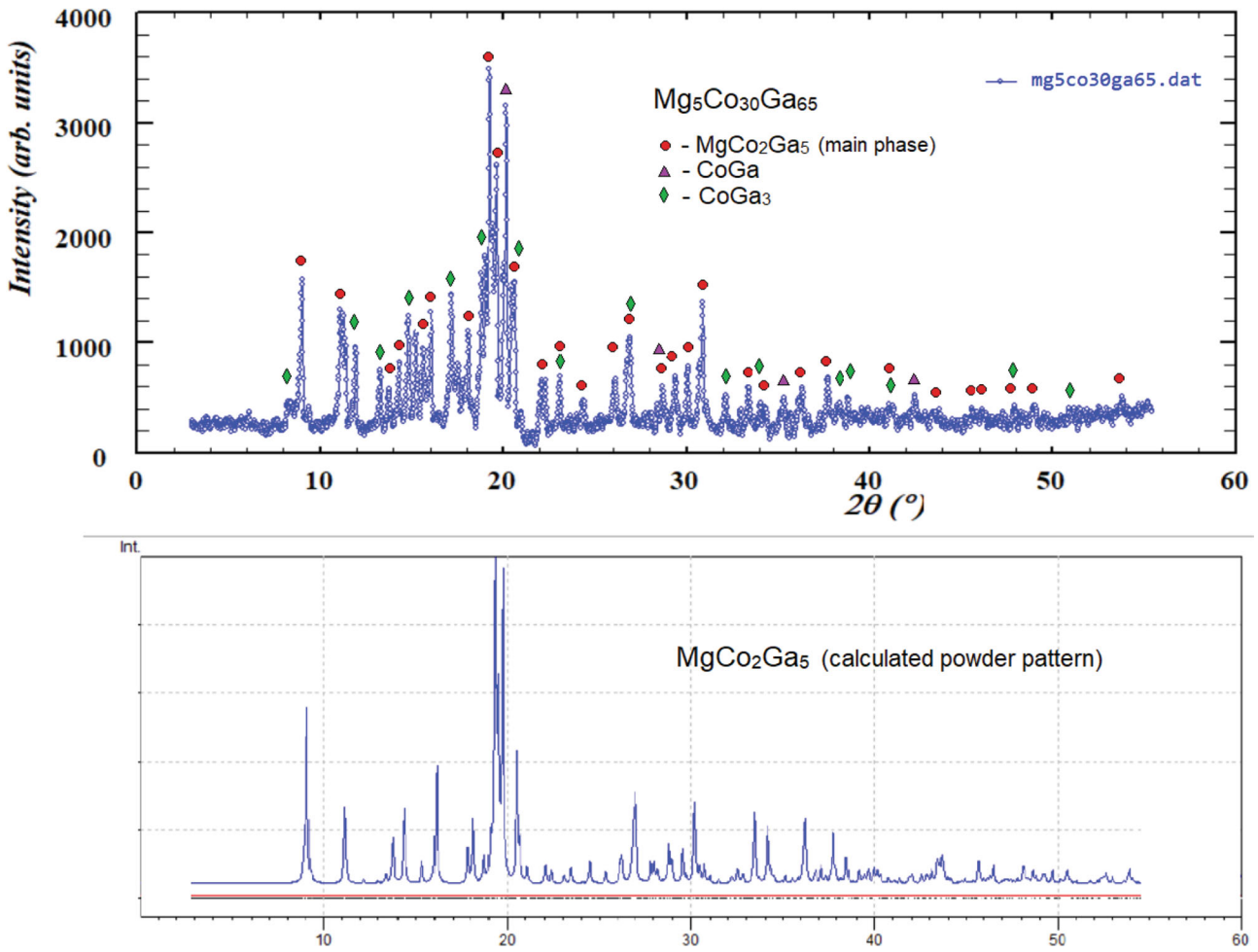

Fig. 5 The observed powder x-ray diffraction patterns (Mo Kα radiation) for the $Mg_5Co_{30}Ga_{65}$ sample and their phase content

homogeneity ranges of all ternary phases slightly extend at a constant Mg-content, originating by a Co/Ga substitution. Studying Mg-Co-Ga system in the whole composition region, we confirmed the existence of five ternary compounds: τ_1—$MgCo_2Ga_5$ (*Pnnm* space group, own structure type), τ_2—$Mg_3Co_2Ga_7$ (*C2/c* space group, own structure type), τ_3—$MgCoGa_2$ ($P2_1/n$ space group, own structure type), τ_4—$Mg_{1-x}Co_{2-y}Ga_{x+y}$ (x = 0.06, y = 0.64) (*Cmcm* space group, own structure type), τ_5—$Mg_{1-x}Co_{2-y}Ga_{x+y}$ (x = 0.10, y = 0.16) (*R*-3 *m* space group, own structure type). In addition, six solid solutions are formed based on binary phases: S_1—$MgCo_{2-x}Ga_x$ (x = 0-1), S_2—$MgGa_{1-x}Co_x$, S_3—$MgGa_{2-x}Co_x$, S_4—$Mg_2Ga_{5-x}Co_x$, S_5—$CoGa_{3-x}Mg_x$ and S_6—$CoGa_{1-x}Mg_x$.

The peculiarity of the Mg-Co-Ga system is the formation of both individual ternary intermetallics and solid solutions based on individual binary phases. The formation of ternary intermetallics is due to the differences in the electronic configurations of the components (Mg is an *s*-element, Co is a *d*-metal, and Ga is a *p*-element). Also, the values of metallic radius and electronegativity of magnesium (metallic radii r_{Mg} = 1.60 Å, electronegativity χ_{Mg} = 1.31) are significantly different from cobalt (r_{Co} = 1.25 Å, χ_{Co} = 1.88) and gallium (r_{Ga} = 1.35 Å, χ_{Co} = 1.81).[21,22] The close values of electronegativities and slight differences in the metallic radii of cobalt and gallium are the reason for the formation of solid solutions due to the mutual substitution of Ga and Co.

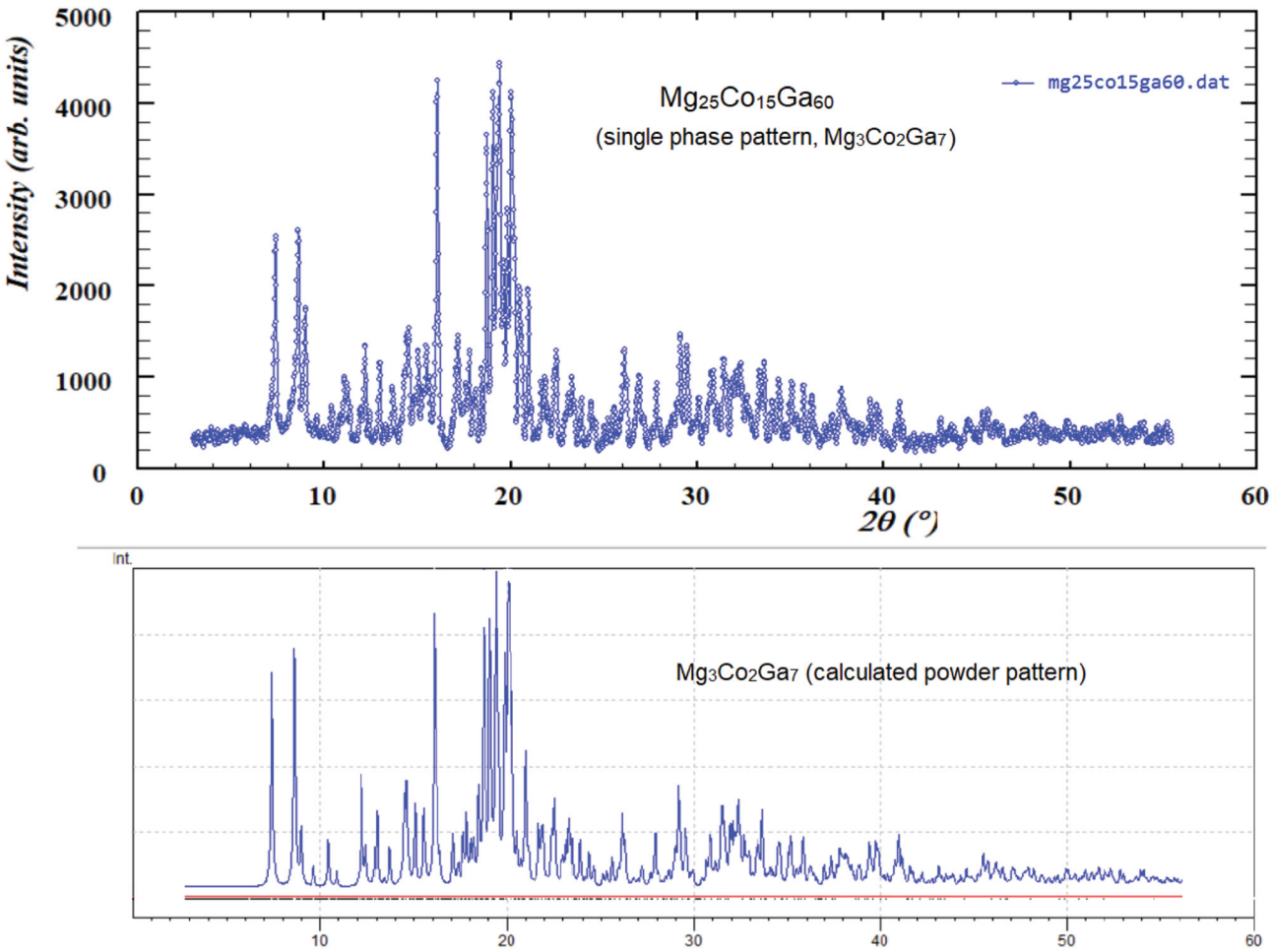

Fig. 6 The observed powder x-ray diffraction patterns (Mo Kα radiation) for the $Mg_{25}Co_{15}Ga_{60}$ sample and their phase content

The most extensive homogeneity ranges are the solid solutions between the binary phases $MgCo_2$ and $MgGa_2$. Under the studied conditions the $MgCo_2$ binary phase dissolves at least 34 at.% Ga and homogeneity region of S_1—$MgCo_{2-x}Ga_x$ (x = 0-1) solid solution phase extends to equiatomic composition MgCoGa. The $MgGa_2$ binary phase dissolves at least 4 at.% Co. The solubility of Co in MgGa and Mg_2Ga_5 binary phase does not exceed 5 at.%. The solubility of Mg in binary phases $CoGa_3$ and CoGa is quite insignificant and does not exceed 2 at.%.

For ternary phases, as well as for solid solutions the crystal structures were determined using modern powder and single crystal apparatus. The results of these structural studies are given below.

4.2 Solid solution on the Base of Binary Compounds

The formation of a hexagonal solid solution S1—$MgCo_{2-x}Ga_x$ (x = 0-1), was found during the investigation of the phase equilibria in the Mg–Co–Ga ternary system at 200 °C. The lattice parameters for alloys from the homogeneity range of this solid solution were determined from structure refinement of single crystal diffraction data. An increase of the lattice parameters *a* and *c* was observed with the increase of gallium content in the alloys. This is since the metallic radius of gallium (r_{Ga} = 1.35 Å) is larger than metallic radius of cobalt (r_{Co} = 1.25 Å).

For more detailed investigation of crystal structure of solid solution $MgCo_{2-x}Ga_x$ the x-ray single crystal

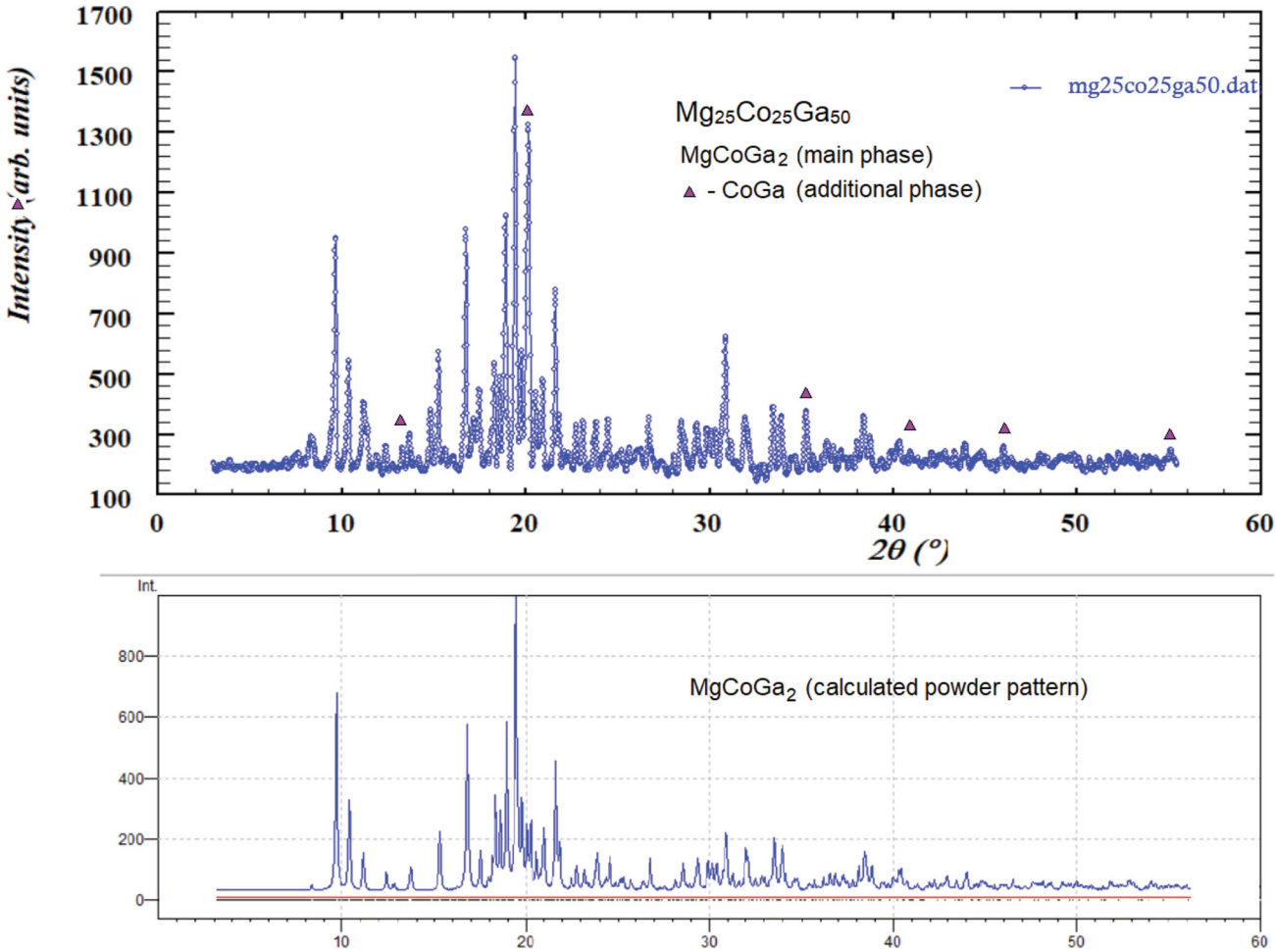

Fig. 7 The observed powder x-ray diffraction patterns (Mo Kα radiation) for the $Mg_{25}Co_{25}Ga_{50}$ sample and their phase content

diffraction was carried out. The structure was solved by direct method. The atom of Mg fully occupies the Wyckoff position 4*f*. Atoms Ga substitute Co in both sites 2*a* and 6 *h*. The crystallographic data and experimental details of these single crystals are shown in Table 3. The refined atomic parameters are presented Table 4. The boundaries of the homogeneity regions for all solid solutions were determined from the change of the unit cell dimensions with the composition of substituted component, which is illustrated in Fig. 9. An increase of the lattice parameters *a* and *c* was observed with the increase of gallium content in the alloys. The maximum solubility of gallium in the binary phase $MgCo_2$ is 34 at.% and the composition of the phase extends to equiatomic MgCoGa.

The crystal structure of S2—$MgGa_{1-x}Co_x$ solid solution phase was determined by single crystal diffraction. The observed structure factors of 602 unique reflections were used for structure solution and refinement. The crystal structure of tetragonal S2—$MgGa_{1-x}Co_x$ was solved by direct methods. In the first stage of structure determination, the two positions (16*f*) of the Mg and Ga atoms were obtained by direct methods. After the refinement of positional, thermal displacement and occupation parameters were obtained showing that one site 16*f* is fully occupied

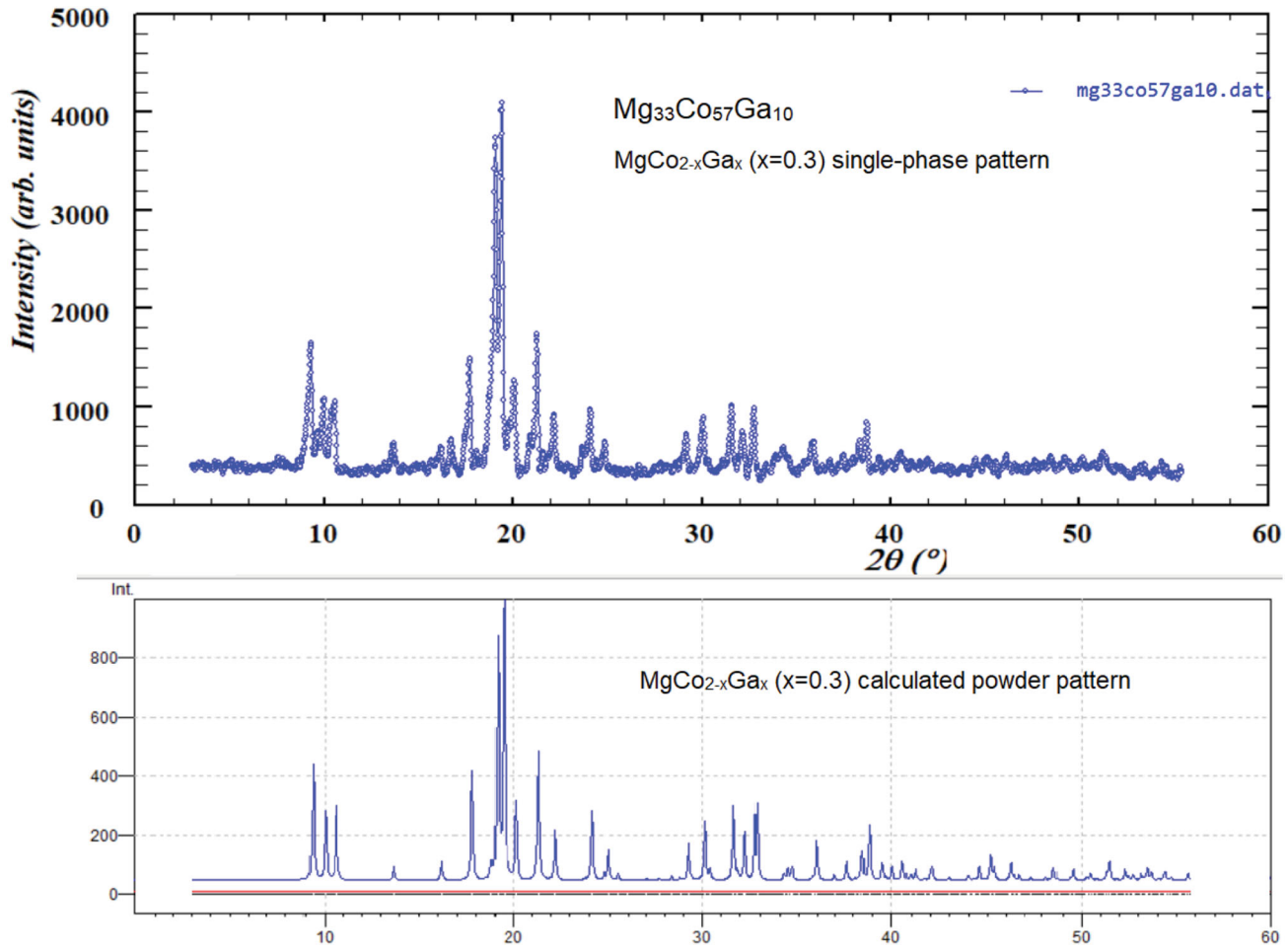

Fig. 8 The observed powder x-ray diffraction patterns (Mo Kα radiation) for the $Mg_{33}Co_{57}Ga_{10}$ sample and their phase content.

by magnesium atoms and second site 16*f* is occupied by statistical mixture of Ga/Co atoms. The crystallographic data and experimental details of these single crystals are shown in Table 3. The refined atomic parameters are presented Table 4. This solid solution does have a small region of homogeneity. The solubility of Co in MgGa does not exceed 3 at.% Ga.

The solid solution S3—$MgGa_{2-x}Co_x$ according to energy/wavelength dispersive spectrometry (EDS/WDS) and x-ray diffraction (XRD) data is limited to 6 at.% Co. A decrease of the lattice parameters *a* and *c* was observed with the increase of gallium content in the alloys (Fig. 10) because the metallic radius of cobalt (r_{Co} = 1.25 Å) is smaller than the metallic radius of gallium (r_{Ga} = 1.35 Å).

Up to 5 at.% cobalt atoms dissolve in Mg_2Ga_5 phase, and formation of S4—$Mg_2Ga_{5-x}Co_x$ is observed. Magnesium-rich binary phases, Mg_5Ga_2 and Mg_2Ga, do not dissolve cobalt atoms.

The solubility of Mg in binary $CoGa_3$ and CoGa phases is insignificant and does not exceed 3 at.%. To establish the mechanism of formation of solid solutions during the dissolution of magnesium atoms in the binary phases of the Co-Ga system, a study of the structure by the single crystal method was carried out using the $CoGa_3$ phase as example. The refinement of positional, thermal displacement and occupation parameters revealed that one site 4*d* is fully occupied by cobalt atoms and one site 4*c* is fully occupied by Ga atoms, and site 8*j* is occupied by statistical mixture

Table 3 Crystal data and structure refinement for $MgCo_2{}_xGa_x$, $MgGa_1{}_xGa_x$ (x = 0.04), (x = 0.70), and $CoGa_3{}_xMg_x$ (x = 0.04)

Empirical formula	$MgCo_{1.30}Ga_{0.70}$	$MgGa_{0.96}Ga_{0.04}$	$CoGa_{2.96}Mg_{0.04}$
Structure type	$MgZn_2$	MgGa	$IrIn_3$
Formula weight, M_r (g/mol)	149.67	93.60	266.25
Diffractometer	Xcalibur Oxford Diffraction	Xcalibur Oxford Diffraction	Xcalibur Oxford Diffraction
Crystal system	hexagonal	tetragonal	tetragonal
Space group	$P6_3/mmc$	$I4_1/a$	$P4_2/mnm$
Pearson symbol, Z	*hP12,* 4	*tI*32,16	*tP*16, 4
Unit cell dimensions:			
a, Å	5.00980(15)	10.5989(9)	6.2533(10)
b, Å			
c, Å	8.0956(3)	5.5511(11)	6.5427(13)
V, Å^3	175.96(3)	623.59(16)	255.84(8)
Calculated density ($D_{calc,}$ g/sm^3)	5.650	3.988	8.913
Absorption coefficient (μ, mm^{-1})	22.698	17.092	36.823
θ range for data collection (deg.)	4.70 ÷ 32.17	3.84 ÷ 35.18	4.51 ÷ 28.22
Range in *h k l*	$-7 \le h \le 7$,	$-14 \le h \le 16$,	$-8 \le h \le 8$,
	$-7 \le k \le 7$,	$-8 \le k \le 8$,	$-8 \le k \le 8$,
	$-11 \le l \le 11$	$-15 \le l \le 15$	$-8 \le l \le 8$
collected/unique	2945/145	5586/602	6758/195
Data/parameters	145/12	602/21	195/13
Goodness-of-fit on F^2	1.31	1.054	1.62
Final *R* indices [$I > 2\sigma(I)$]	R_1 = 0.0333;	R_1 = 0.0127;	R_1 = 0.0303;
	wR_2 = 0.0882	wR_2 = 0.0275	wR_2 = 0.0743
R indices (all data)	R_1 = 0.0372;	R_1 = 0.0168;	R_1 = 0.0304;
	wR_2 = 0.0910	wR_2 = 0.0287	wR_2 = 0.0744
$\Delta\rho_{fin}$ (max/min), e·Å^{-3}	2.07 and − 1.39	0.28 and − 0.42	1.20 and − 2.04

of Ga/Mg atoms in ratio 0.98/0.02. The crystallographic data and experimental details of S5—$CoGa_{3-x}Mg_x$ (x = 0.04) single crystal are shown in Table 3. The refined atomic parameters are presented Table 4. These data prove that the formation of S5—$CoGa_{3-x}Mg_x$ S6—$CoGa_{1-x}Mg_x$ solid solutions occurs by partial substitution of gallium atoms by magnesium.

4.3 Ternary Compounds

This section describes the crystal structure of all ternary phases of the Mg-Co-Ga system. The crystal structures of all ternary compounds have been investigated by us using the single crystal method and have been published or are in print in scientific journals specializing in the description of crystal structures. Therefore, only the basic structural characteristics are given in this section, and complete structural data are available from cited literature.

The τ_1–$MgCo_2Ga_5$ is new structure type with orthorhombic symmetry, space group *Pnnm*, lattice parameters: *a* = 6.2700(2) Å, *b* = 6.6946(2) Å, *c* = 6.0789(2) Å and contains 16 atoms per unit cell.[5] This structure is closely related to the tetragonal binary $CoGa_3$ phase,[23,24] which crystallizes in high-temperature *ht*-$IrIn_3$ structure type (space group $P4_2/mnm$). The orthorhombic structure of ternary $MgCo_2Ga_5$ is derived from binary $CoGa_3$ phase via a *translationengleiche* symmetry reduction of index 2. According to the Bärnighausen scheme,[25] the symmetry reduction from $P4_2/mnm$ to *Pnnm* splits the 4*c* site into two sites 2*a* and 2*b*. Positional atomic parameters, occupation of sites, and thermal displacement parameters are presented in Table 5.

Table 4 Fractional atomic coordinates, isotropic or equivalent isotropic and anisotropic displacement parameters (Å^2) for solid solution $MgGa_{1-x}Ga_x$ (x = 0.04), $MgCo_{2-x}Ga_x$ (x = 0.70), and $CoGa_{3-x}Mg_x$ (x = 0.04) phases

Atoms	Sites	*x/a*	*y/b*	*z/c*	U_{iso}*/U_{eq}	Occ. (<1)
$MgCo_{2-x}Ga_x$ (x = 0.70)						
Mg	*4f*	1/3	2/3	0.5667 (4)	0.0065(7)	
(Co/Ga)1	*2a*	0	0	0	0.0081(5)	0.75/25
(Co/Ga)2	*6 h*	0.17214(11)	0.3443(2)	1/4	0.0069(5)	0.62/38

	U^{11}	U^{22}	U^{33}	U^{12}	U^{13}	U^{23}
Mg	0.0071(10)	0.0071(10)	0.0054(15)	0.0036(5)	0.000	0.000
(Co/Ga)1	0.0115(6)	0.0115(6)	0.0013(8)	0.0058(3)	0.000	0.000
(Co/Ga)2	0.0079(5)	0.0065(6)	0.0058(6)	0.0032(3)	0.000	0.000

Atoms	Sites	*x/a*	*y/b*	*z/c*	U_{iso}*/U_{eq}	Occ. (<1)
$MgGa_{1-x}Ga_x$ (x = 0.04)						
Mg	*16f*	0.63180(4)	0.32345(4)	− 0.35649(7)	0.01819(10)	
Co/Ga	*16f*	0.697791(10)	0.358960(12)	0.13098(2)	0.01564(6)	0.96/0.04

	U^{11}	U^{22}	U^{33}	U^{12}	U^{13}	U^{23}
Mg	0.02159(19)	0.01767(18)	0.01533(19)	0.00370(14)	− 0.00090(14)	0.00185(14)
Co/Ga	0.01443(8)	0.01953(8)	0.01297(9)	− 0.00010(4)	0.00010(4)	− 0.00171(4)

Atoms	Sites	*x/a*	*y/b*	*z/c*	U_{iso}*/U_{eq}	Occ. (<1)
$CoGa_{3-x}Mg_x$ (x = 0.04)						
(Ga/Mg)1	*8j*	0.34444(9)	0.34444(9)	0.76236(13)	0.0017(4)*	0.98/0.02
Ga2	*4c*	1/2	0	1/2	0.0030 (4)	
Co	*4d*	0.15640(16)	0.15640(16)	1/2	0.0032 (5)	

	U^{11}	U^{22}	U^{33}	U^{12}	U^{13}	U^{23}
Ga2	0.0017(6)	0.0045(6)	0.0028(6)	0.0011(4)	0.000	0.000
Co	0.0037(5)	0.0037(5)	0.0021(8)	− 0.0001(4)	0.000	0.000

The τ_2–$Mg_3Co_2Ga_7$[6] is a new structure type: monoclinic space group *C*2/*c*, *a* = 9.0873(9) Å, *b* = 9.4598(9) Å, *c* = 9.4361(9) Å, β = 93.605(8), V = 809.5(1) Å^3. The structure has no close analogues among the known types of intermetallic compounds. Considering the coordination of atoms, this structure can be attributed to class 9, according to the Krypyakevich classification scheme.[26]

The crystal structure τ_3–$MgCoGa_2$[7] can be described in two space groups as $P2_1/c$ (standard setting) and $P2_1/n$ (non-standard setting) with lattice parameters for the standard setting: *a* = 5.1505(2), *b* = 7.2571(2), *c* = 8.0264(3) Å, β = 125.571(3) , and for the non-standard setting: *a* = 5.1505(2), *b* = 7.2571(2), *c* = 6.5464(2) Å, β = 94.217(3) . The crystal structure is related to other similar structures, such as YPd_2Si and Fe_3C. The $MgCoGa_2$ structure is derived from Fe_3C via a *translationengleiche (t)* symmetry reduction of index 2.

The τ_4–$Mg_{1-x}Co_{2-y}Ga_{x+y}$ (x = 0.06, y = 0.64)[8] is orthorhombic with space group *Cmcm* (*a* = 4.9868(9), *b* = 25.959(4), *c* = 8.0508(11) Å). The structure of this compound is closely related to Laves phases $MgZn_2$ ($P6_3/mmc$) and URe_2 (*Cmcm*). According to Bärnighausen formalism, from hexagonal phase $MgZn_2$ via a *translationengleiche* symmetry reduction of index 3 (t3) results in orthorhombic structure URe_2. Phase τ_3–$Mg_{1-x}Co_{2-y}Ga_{x+y}$ derives from an orthorhombic URe_2 via *klassengleiche* subgroups (a, 3b, c).

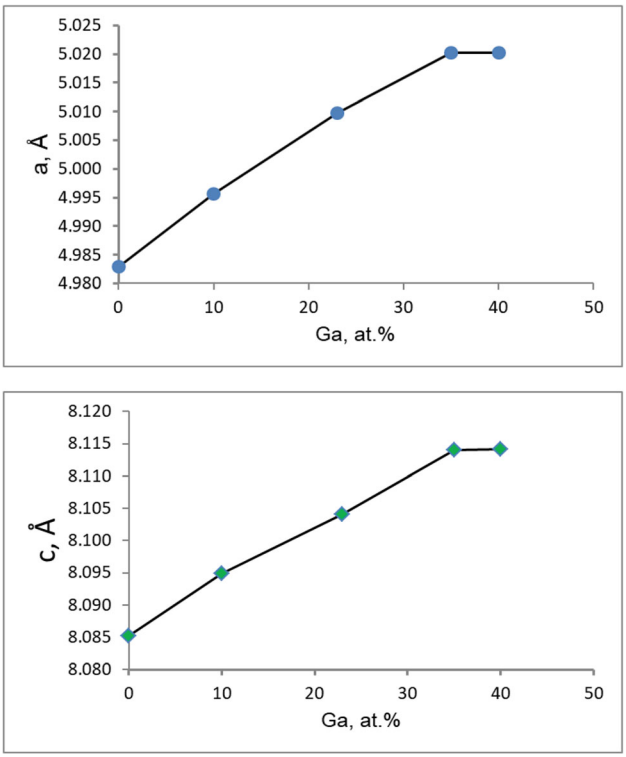

Fig. 9 Changes of unit cell dimensions for $MgCo_{2-x}Ga_x$ solid solution phase

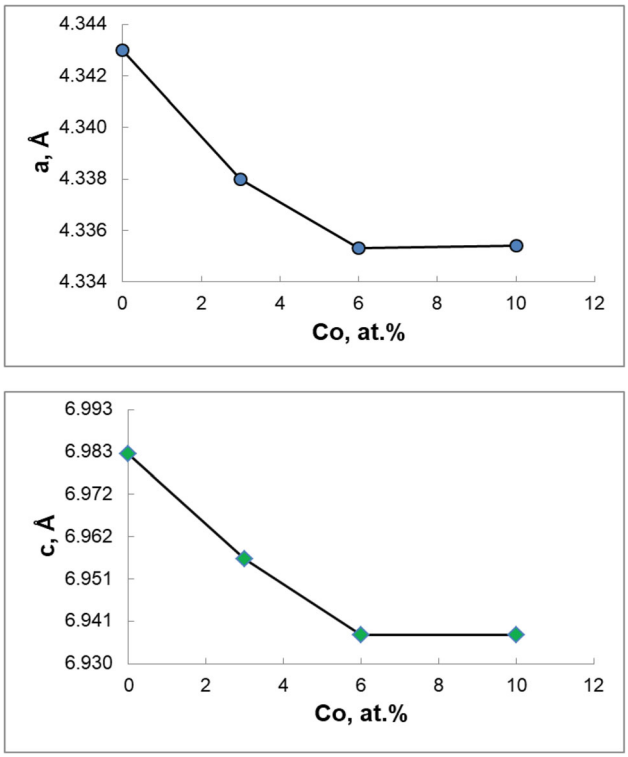

Fig. 10 Changes of unit cell dimensions for $MgGa_{2-x}Co_x$ solid solution phase

The structure of trigonal phase τ_5–$Mg_{1-x}Co_{2-y}Ga_{x+y}$ (x = 0.10, y = 0.16)[8] with space group *R*-3 *m* (*a* = 4.9296(2), *c* = 12.0744(7) Å) is strongly disordered. The average structure consists of two subcells with ratio 9:1. Subcell A is closely related to $MgZn_2$-type. The subcell B is a hypothetical $CoGa_5$ structure which has no close analogs among known structural types.

The τ_4–$Mg_{1-x}Co_{2-y}Ga_{x+y}$ (x = 0.06, y = 0.64) and τ_5–$Mg_{1-x}Co_{2-y}Ga_{x+y}$ (x = 0.10, y = 0.16) compounds belong to the Laves phase family. In general, binary Laves phases are given in the 1:2 components ratio, for example, $MgCo_2$ ($MgZn_2$-type), therefore the formula of the ternary Laves phases from the Mg-Co-Ga system are given as $MgCo_{2-x}Ga_x$ (S_1), τ_4—$Mg_{1-x}Co_{2-y}Ga_{x+y}$ (x = 0.06, y = 0.64) and τ_5—$Mg_{1-x}Co_{2-y}Ga_{x+y}$ (x = 0.10, y = 0.16). Since in the τ_4 and τ_5 structures Mg atoms do not completely occupy the sites the value of *x* shows how much the composition of phases is shifted from the ideal composition of Laves phases.

5 Summary

The isothermal section of Mg-Co-Ga phase diagram was studied in the whole composition range. Phase relations of this system were determined at 200 °C by characterizing about 60 ternary alloys. Five ternary compounds: τ_1—$MgCo_2Ga_5$ (*Pnnm* space group, own structure type), τ_2—$Mg_3Co_2Ga_7$ (*C2/c* space group, own structure type), τ_3—$MgCoGa_2$ ($P2_1/n$ space group, own structure type), τ_4—$Mg_{1-x}Co_{2-y}Ga_{x+y}$ (x = 0.06, y = 0.64) (*Cmcm* space group, own structure type), τ_5—$Mg_{1-x}Co_{2-y}Ga_{x+y}$ (x = 0.10, y = 0.16) (*R*-3 *m* space group, own structure type) form in this system. For all ternary compounds crystal structures were investigated by means of single crystal diffraction. In addition to ternary compounds, solid solutions based on binary phases are formed in the system. The formation of ternary intermetallics is due to differences in the electronic configuration of the components, electronegativity and metallic radius of Mg, Co and Ga.

Table 5 Fractional atomic coordinates, isotropic or equivalent isotropic and anisotropic displacement parameters (Å^2) for ternary compounds from Mg-Co-Ga system.

Atoms	Sites	*x/a*	*y/b*	*z/c*	U_{iso}*/U_{eq}	Occ.
τ_1—$MgCo_2Ga_5$, [5] *Pnnm, a = 6.2700(2) Å, b = 6.6946(2) Å, c = 6.0789(2) Å*						
Mg	2*b*	0	0	1/2	0.0162(8)	1.00
Co	4*g*	0.33958(16)	0.13990(15)	0	0.0112(3)	1.00
Ga1	2*a*	0	0	0	0.0180(4)	1.00
Ga2	8*h*	0.14551(10)	0.34316(10)	0.25337(10)	0.0161(3)	1.00
τ_2—$Mg_3Co_2Ga_7$,[6] *C2/c, a = 9.0873(9) Å, b = 9.4598(9) Å, c = 9.4361(9) Å, β = 93.605(8)*						
Mg1	8*f*	0.1925(2)	0.4474(2)	0.3026(2)	0.011(1)	1.00
Mg2	4*e*	1/2	0.3522(2)	3/4	0.011(1)	1.00
Co1	8*f*	0.2424(1)	0.2731(1)	0.8554(1)	0.009(1)	1.00
Ga1	8*f*	0.2228(1)	0.3317(1)	0.6019(1)	0.009(1)	1.00
Ga2	8*f*	− 0.0644(1)	0.3718(1)	0.4821(1)	0.008(1)	1.00
Ga3	8*f*	0.3781(1)	0.5677(1)	0.5259(1)	0.008(1)	1.00
Ga4	4*e*	0	0.2290(1)	3/4	0.010(1)	1.00
τ_3—$MgCoGa_2$,[7]*a = 5.1505(2), b = 7.2571(2), c = 8.0264(3) Å, β = 125.571(3)*						
Mg	4*e*	0.1827(3)	0.04414(19)	0.2985(2)	0.0049(3)	1.00
Co	4*e*	0.28699(13)	0.39736(8)	0.19208(8)	0.00378(14)	1.00
Ga1	4*e*	0.21859(10)	0.72437(6)	0.08003(7)	0.00448(13)	1.00
Ga2	4*e*	0.38498(11)	0.14078(6)	0.03372(7)	0.00476(13)	1.00
τ_4—$Mg_{1-x}Co_{2-y}Ga_{x+y}$ (x = 0.10, y = 0.16),[8] *Cmcm, a = 4.9868(9), b = 25.959(4), c = 8.0508(11) Å*						
Co1	3*a*	0	0	0	0.0114(7)	1.00
Co2	9*d*	5/6	2/3	1/6	0.0065(5)*	0.893
Mg1	6*c*	1/3	2/3	0.0404(4)	0.0095(10)*	0.896
Ga1	18 *h*	0.668(2)	0.8342(12)	0.1676(10)	0.009(2)*	0.067
Ga2	6*c*	1/3	2/3	-0.0104(17)	0.006(4)*	0.071
τ_5—$Mg_{1-x}Co_{2-y}Ga_{x+y}$ (x = 0.06, y = 0.64),[8] *R-3m, a = 4.9296(2), c = 12.0744(7) Å*						
(Co/Ga)1	4*c*	0	0.60972(10)	1/4	0.0069(8)	0.68/32
(Co/Ga)2	4*c*	0	0.94270(11)	1/4	0.0052(8)	0.80/20
(Co/Ga)3	4*c*	0	0.27584(11)	1/4	0.0069(7)	0.68/32
(Co/Ga)4	4*a*	0	0	0	0.0062(7)	0.68/32
(Co/Ga)5	8*f*	0	0.33331(8)	− 0.0006(2)	0.0074(4)	0.70/0.30
(Co/Ga)6	8 *g*	0.2570(5)	0.02856(7)	1/4	0.0072(5)	0.64/36
(Co/Ga)7	8 *g*	0.2580(4)	0.36201(7)	1/4	0.0075(6)	0.62/38
(Co/Ga)8	8 *g*	0.2429(4)	0.19529(7)	1/4	0.0074(5)	0.62/38
Mg1	8*f*	0	0.11103(16)	0.0649(8)	0.0043(13)	1.00
Mg2	8*f*	0	0.44471(17)	0.0654(7)	0.0066(13)	1.00
Mg	8*f*	0	0.22209(17)	0.5662(6)	0.0095(11)*	0.94
Ga	8*f*	0	0.22209(17)	0.5662(6)	0.0095(11)*	0.06

Close values of electronegativities and slight differences in metallic radii between Co and Ga are the reason for the formation of solid solutions due to the mutual substitution of Ga and Co. The largest area of homogeneity is observed for the solid solution S1—$MgCo_{2-x}Ga_x$ (x = 0-1, *P6$_3$/mmc* space group, $MgZn_2$ structure type). The solubility of Mg in binary phases from Co-Ga systems is rather small, since magnesium differs in atomic size and electronic structure from the other atoms in this system.

Acknowledgements Financial support from the National Science Centre, Poland (No 2017/25/B/ST8/02179) and German Academic Exchange Service (DAAD) is gratefully acknowledged (No 91774331, bilateral PhD scholarship grant). Partial financial support from Simons Foundation (Award Number: 1037973) is also gratefully acknowledged.

References

1. M. Dornheim, S. Doppiu, G. Barkhordarian, U. Boesenberg, T. Klassen, O. Gutfleisch, and R. Bormann, Hydrogen Storage in Magnesium-Based Hydrides and Hydride Composites, *Scr. Mater.*, 2007, **56**, p 841–846.
2. B. Reiser, and K. Bogdanovic, Schlichte, The Application of Mg-Based Metal-Hydrides as Heat Energy Storage Systems, *Int. J. Hydrog. Energy*, 2000, **25**, p 425–430.

3. J.-C. Crivello, R.V. Denys, M. Dornheim, M. Felderhoff, D.M. Grant, J. Huot, T.R. Jensen, P. de Jongh, M. Latroche, G.S. Walker, C.J. Webb, and V.A. Yartys, Mg-Based Compounds for Hydrogen and Energy Storage, *Appl. Phys. A*, 2016, **122**, p 85.
4. F. Bella, S. De Luca, L. Fagiolari, D. Versaci, J. Amici, C. Francia, and S. Bodoardo, An Overview on Anodes for Magnesium Batteries: Challenges Towards a Promising Storage Solution for Renewables, *Nanomaterials*, 2021, **11**(3), p 810.
5. N. Pavlyuk, G. Dmytriv, V. Pavlyuk, B. Rożdżyńska-Kiełbik, A. Gil, I. Chumak, and H. Ehrenberg, New Ternary MgCo2Ga5 and MgNi2Ga5 Gallides, *Zeitschrift für Kristallographie Cryst. Mater.*, 2020, **8**, p 17.
6. V. Pavlyuk, B. Marciniak, I. Chumak, E. Różycka-Sokołowska, W. Prochwicz, and J. Kończyk, Crystal Structure of New Intermetallic Compound $Mg_3Co_2Ga_7$, *J. Alloy Compd.*, 2007, **442**, p 96.
7. N. Pavlyuk, G. Dmytriv, V. Pavlyuk, B. Rozdzynska-Kielbik, W. Nitek, W. Lasocha, I. Chumak, and H. Ehrenberg, A New Monoclinic Structure type for Ternary Gallide $MgCoGa_2$, *Acta Crystallogr. Sect. C Struct. Chem.*, 2020, **76**, p 541–546.
8. N. Pavlyuk, G. Dmytriv, V. Pavlyuk, W. Ciesielski, B. Rozdzynska-Kielbik, S. Indris, and H. Ehrenberg, A New Ternary Derivative of the Laves Phases in the Mg-Co-Ga System, *Acta Cryst. B.*, 2023, **B79**, p 255–262.
9. *Binary Alloy Phase Diagrams*, 2nd edn., ed. by T.B. Massalski (ASM International, Materials Park, OH, 1990).
10. A.A. Nayeb-Hashemi, and J.B. Clark, The Ga-Mg (Gallium–Magnesium) System, *Bull. Alloy Phase Diagr.*, 1985, **6**(5), p 434–439.
11. P. Feschotte, and K. Yvon, Stoichiometric Study of Intermediate Compounds in the Gallium–Magnesium System, *J. Less Common Met.*, 1990, **158**, p 89–97.
12. H. Okamoto, Ga-Mg (Gallium–Magnesium), *J. Phase Equilib. Diffus.*, 1991, **12**(1), p 119–120.
13. H. Okamoto, Ga-Mg (Gallium–Magnesium), *J. Phase Equilib. Diffus.*, 2013, **34**, p 148.
14. H. Okamoto, Co-Ga (Cobalt–Gallium), *J. Phase Equilib. Diffus.*, 2005, **26**, p 197.
15. A.A. Nayeb-Hashemi, and J.B. Clark, The Co-Mg (Cobalt–Magnesium) System, *Bull. Alloy Phase Diagr.*, 1987, **8**, p 352–355.
16. X. Su, and J.-C. Tedenac, Thermodynamic Modeling of the Cobalt–Gallium System, *Intermetallics*, 2005, **13**, p 467–473.
17. L.-F. Yang, X.-D. Si, H.-Q. Zhang, F.-Y. Gao, Y.-P. Zheng, Y.-L. Liu, Y.-R. Wang, and Y. Du, Thermodynamic Assessment of the Co-Mg Binary System, *J. Min. Metall. B*, 2022, **58**, p 109–115.
18. M. Notin, B. Belbacha, J. Charles, and J. Hertz, New Experimental Results and Improvement of the Modelization of the (Ga, Mg) System, *J. Alloys Compd.*, 1991, **176**, p 25–38.
19. Oxford Diffraction, *CrysAlis CCD and CrysAlis RED*. Oxford Diffraction Ltd., Cambridge, 2008.
20. G.M. Sheldrick, *SHELXL-97. Program for Crystal Structure Refinement*. University of Göttingen, Göttingen, 1997.
21. L. Pauling, The Nature of the Chemical Bond. IV. The Energy of Single Bonds and the Relative Electronegativity of Atoms, *J. Am. Chem. Soc.*, 1932, **54**(9), p 3570–3582.
22. J.C. Slater, Atomic Radii in Crystals, *J. Chem. Phys.*, 1964, **41**(10), p 3199–3204.
23. P. Viklund, S. Lidin, P. Berastegui, and U. Häussermann, Variations of the $FeGa_3$ Structure Type in the Systems $CoIn_{3-x}Zn_x$ and $CoGa_{3-x}Zn_x$, *J. Solid State Chem.*, 2002, **165**, p 100–110.
24. R. Pöttgen, R.-D. Hoffmann, and G. Kotzyba, Structure, chemical bonding, and properties of $CoIn_3$, $RhIn_3$, and $IrIn_3$, *Z. Anorg. Allg. Chem.*, 1998, **624**, p 244.
25. H. Bärnighausen, Group-Subgroup Relations Between Space Groups: A Useful Tool in Crystal Chemistry, *Commun. Math. Chem.*, 1980, **9**, p 139–175.
26. P.I. Krypyakevich, The structural types of the intermetallic compounds, *Nauka*, 1977, p 287.